SEGMENTATION-FREE MEASUREMENT OF CORTICAL THICKNESS FROM MRI

By

Iman Aganj

Guillermo Sapiro

Neelroop Parikshak

Sarah K. Madsen

and

Paul M. Thompson

IMA Preprint Series # 2181

(November 2007)

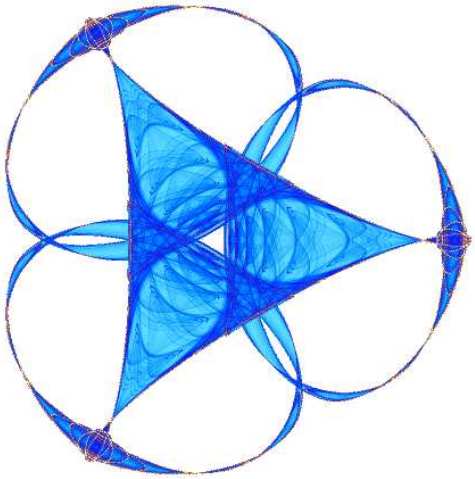

INSTITUTE FOR MATHEMATICS AND ITS APPLICATIONS

UNIVERSITY OF MINNESOTA

400 Lind Hall

207 Church Street S.E.

Minneapolis, Minnesota 55455–0436

Phone: 612-624-6066 Fax: 612-626-7370

URL: http://www.ima.umn.edu

SEGMENTATION-FREE MEASUREMENT OF CORTICAL THICKNESS FROM MRI

Iman Aganj,[1] Guillermo Sapiro,[1] Neelroop Parikshak,[2] Sarah K. Madsen,[2] and Paul M. Thompson[2]

[1] Department of Electrical and Computer Engineering, University of Minnesota, Minneapolis, MN 55455, USA

[2] Laboratory of Neuro Imaging, University of California-Los Angeles, School of Medicine, Los Angeles, CA 90095, US

ABSTRACT

Estimating the thickness of cerebral cortex is a key step in many MR brain imaging studies, revealing valuable information on development or disease progression. In this work we present a new approach to measure the cortical thickness, based on minimizing line integrals over the probability map of the gray matter in the MRI volume. Previous methods often perform a binary-valued segmentation of the gray matter before measuring the thickness. Because of image noise and partial voluming, such a hard classification ignores the underlying tissue class probabilities assigned to each voxel, discarding potentially useful information. We describe our proposed method and demonstrate its performance on both artificial volumes and real 3D brain MRI data from subjects with Alzheimer's disease and healthy individuals.

***Index Terms*—** Cortical thickness measurement, gray matter density, magnetic resonance imaging, soft classification.

1. INTRODUCTION

Measuring the cortical thickness has long been a topic of interest for neuroscientists. Cortical thickness changes in a characteristic pattern during childhood development and with the progression of neurodegenerative diseases such as Alzheimer's, HIV/AIDS, and epilepsy [1]–[2]. Recent studies examining changes in cortical thickness over time have revealed the trajectory of diseases in the living brain, and have been used to quantify treatment effects, identifying regions where cortical thickness correlates with age, cognitive deterioration, genotype, or medication.

Various approaches have recently been proposed to automate this cortical thickness measurement from Magnetic Resonance Imaging (MRI) data, e.g., [3]–[10]. The limited spatial resolution of most MRI volumes (typically 1-2 mm) makes it difficult to measure cortical thickness accurately, which varies from 2 to 5 mm in different brain regions and is only a few voxels thick in the images. The neuroscience community has not yet agreed on a unique definition of cortical thickness and so far various proposed methods measure slightly different quantities. What is common among them is that they virtually all perform a pre-segmentation of the white matter (WM), gray matter (GM), and cerebrospinal fluid (CSF), and most extract explicit models of the surfaces between them (i.e., the inner surface between WM and GM and outer surface between GM and CSF). They then use this hard segmentation as the input data for different tissue thickness measurement algorithms (Sec. 2 briefly reviews previous work). The disadvantage of this approach is that in the hard segmentation process, a considerable amount of information is discarded and never used in measurement, not to mention the significant error in measured thickness that could be introduced by a few misclassified voxels (see Sec. 4.1 for an example).

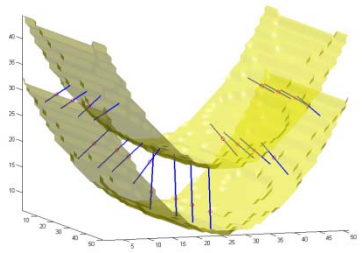

Fig. 1. *Results on an artificial probability map. Inner and outer surfaces of a paraboloid-shaped layer of GM are depicted. Line segments are chosen by the algorithm such that they give the smallest integrals (of the probability map) among all line segments passing through every selected test point, shown as small circles.*

The approach we adopt here uses a soft pre-labeled volume as the input data. Due to the limited resolution of an MRI volume, many voxels contain partial amounts of two or more tissue types (see [11] and the references therein). Their intensity values give us information about the probability/proportion of those voxels belonging to any of the categories of WM, GM, or CSF. Rather than a pre-classified volume, we use one containing the probability that each voxel belongs to the GM.[1] These probability values have the same precision as the values in the original MRI volume, and therefore we do not discard any useful information. We compute line integrals of the soft classified data, centered at each voxel and in all possible spatial directions, and then consider their minimum as the local cortical thickness at that voxel (Fig.1).

In Sec. 2 we review previous work on cortical thickness measurement. Sec. 3 describes our proposed framework, and experimental results are presented in Sec. 4. Sec. 5 concludes with a review of the contributions.

2. PREVIOUS WORK

We now discuss some of the previously reported work for measuring the cortical thickness. Most methods require a pre-segmentation of the inner and outer surface, which results in a loss of available information and often inaccuracy of the input to the main measuring algorithm.

[1] When considering partial volume effects, these "probabilities" represent the proportion of GM in the voxel.

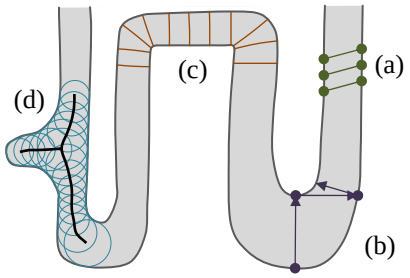

Fig. 2. *Common ways of measuring cortical thickness. (a) Coupled surface methods. (b) Closest point methods. (c) Laplace ('heat-flow') methods. (d) Largest enclosed sphere methods.*

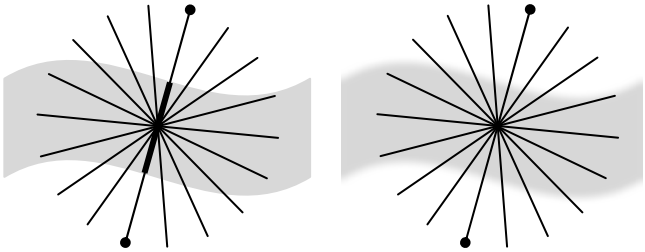

Fig. 3. *Computing line integrals passing through a point, and choosing the minimum integral value. (a) Binary probability map. (b) Continuous probability map.*

Coupled surface methods [3], [12], define the cortical thickness as the Euclidean distance between corresponding point pairs on the inner and outer surfaces, often with parametric grids imposed. A displaced surface may result in an overestimation of the thickness (see Fig. 2(a)). *Closest point methods* such as [13] compute for each point on one of the two surfaces the closest point on the other surface and define the thickness as the distance between them. The main drawback to these methods is the absence of symmetry, as seen in Fig. 2(b). In another method introduced in [14], the *regional histogram of thickness* is estimated by measuring the length of the line segments connecting the inner and outer surfaces of the GM layer, normal to one of the surfaces. The median of the histogram is then chosen as the local cortical thickness. A detection of the WM-GM and GM-CSF boundaries is however necessary.

Laplace Methods [4], [7], [15] solve Laplace's equation in the GM region with the boundary condition of constant (but different) potentials on each of the two surfaces. The cortical thickness is then defined on each point as the length of the integral curve of the gradient field passing through that point, as illustrated in Fig. 2(c). With this approach, the thickness is uniquely defined at every point. Nevertheless, a pre-segmentation of the two surfaces is required, reducing the accuracy of this technique.

Another category of methods defines thickness by making use of a central axis or skeleton [9], [16]. Thickness is typically estimated as the diameter of the largest enclosed sphere in the GM layer, which is (in some cases only initially) centered on a point on the central axis. As Fig. 2(d) demonstrates, a relatively sharp change in the thickness may result in a new branch and affect the topology of the skeleton.

The vast majority of the methods reported in the literature propagate segmentation errors to later steps, and segmentation is still in itself a challenging problem in brain imaging. Considering that the GM layer spans only a few voxels at the commonly used 1-2 mm resolutions, these errors can be significant, and measuring tissue thickness avoiding this hard segmentation step may be very beneficial. This is the approach introduced here and described next.

3. METHODS

3.1. Definition

In its simplest form, we define the thickness of the GM at a given voxel as the minimum line integral of the probability map of the GM over all lines passing through that voxel. Formally:

$$T(\vec{x}) \coloneqq \min_{l \in L_{\vec{x}}} \int_l P(\vec{r}) dl,$$

where $T(\vec{x})$ is the thickness of the GM at a point $\vec{x} \in \mathbb{R}^3$, $P(\vec{x})$ is the probability of the point $\vec{x}$ belonging to the GM (estimation of this probability is described in Sec. 4.2), and $L_{\vec{x}}$ is the set of all lines in three-dimensional space passing through the point $\vec{x}$. In practice, however, $L_{\vec{x}}$ is comprised of all equal-length *line segments* centered at $\vec{x}$, which are sufficiently longer than the expected maximum thickness in the volume. Choosing longer line segments does not greatly affect the integral values since $P(\vec{r})$ decreases significantly on the non-GM regions. Fig. 3(a) shows an example of this construction for a 2D binary probability map, where the probability of belonging to the GM is 1 inside the shape and 0 outside. When computing thickness at the specified point, the line segment marked with oval arrows is selected as the one giving the smallest line integral. The corresponding integral value, which in this case is the length of its overlap with the GM (in bold), is the thickness of the GM at that point. A more realistic situation is shown in Fig. 3(b), where the probability map varies between zero and one. A blurred border, which results from the limited resolution of the MRI, includes voxels that partially contain GM. Due to the pre-segmentation, this type of partial volume information is not considered in most prior work in this area.

Our method is based on an intuitive way of measuring the thickness of an object. A simple way to measure the local thickness of an object would be to put two fingers on both edges of the object, and move the finger tips locally (equivalent to varying the angle of the segment connecting them to each other), until the distance between them is minimized. This distance could then be considered as the local thickness of the object. Thus, we are dealing with a constrained optimization problem: minimizing a distance in a specific region. In our approach, however, this region is identified precisely by a point where we want to define the thickness. Therefore the constraint is that the point must be on the line segment connecting the two finger tips, in other words we consider only the line segments passing through the point where we intend to find the thickness. The minimized distance – or the length of the line segment – is in this case the integral of the probability map on the line containing the segment.

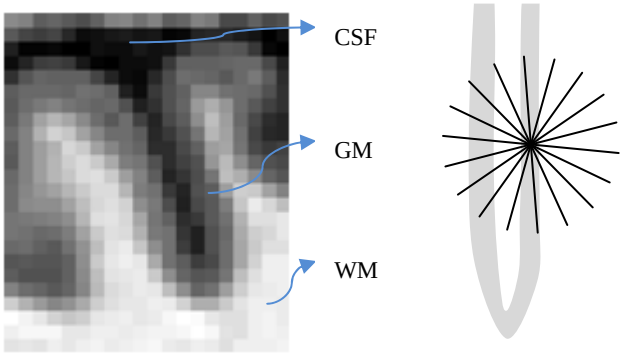

Fig. 4. *(a) A sulcus in which two sides of the gray matter layer are close to each other. (b) How the algorithm might overestimate the thickness if no stopping criteria were used.*

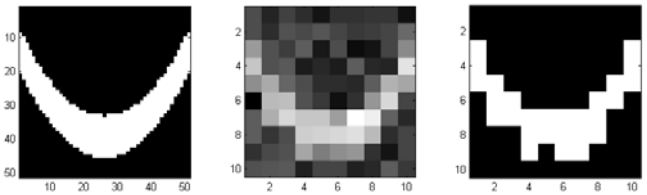

Fig. 5. *(a) A 2D slice of the volume presented in Fig. 1. (b) The same slice in a five-times-lower-resolution volume with additive Gaussian noise. (c) Binary classification of the low-resolution volume.*

3.2. Algorithm

The algorithm basically computes every line integral centered at each point of the volume starting from that point and proceeding in each of the two opposite directions separately. Once all the line integrals at a point are calculated (meaning in all possible directions), the minimum of them is considered to be the thickness on that point. However, to reduce the effect of noise, an alternative would be for instance to consider the average of some of the smallest integrals.

In practice, a problem may arise typically in narrow sulci where the outer surface of the folded GM layer has two nearby sides (Fig. 4(a)). While computing the thickness on one part of the layer, the GM of the other part may be partially included in some of the line integrals; this may lead to the thickness being overestimated (Fig. 4(b)). To avoid this error, we include two stopping criteria which prevent a line integral from further advancing when it is believed that no more summation is necessary or that we are mistakenly considering a different region of the GM layer. The line integral stops proceeding if the probability map:

1. Has been below a specific threshold for a certain number of consecutive voxels, or

2. Has been decreasing at least for a certain number of successive voxels and then increasing for an additional number of voxels.

We use the first criterion, since if the probability has been low for a while, we are most likely not in the GM region anymore, and by further summing we would just increase the error. An additional advantage of using this stopping criterion is that summation will be stopped quickly after starting to measure the thickness on voxels that are not in the GM region, as if the algorithm is ignoring those points and so it returns almost zero values as the GM thickness on them.

The second condition happens when two parts of the GM layer are so close to each other that the probability on the gap between them is not small enough for the first stopping condition to become true, therefore the algorithm stops summing after identifying a valley on the probability map. The algorithm can be implemented such that gaps as narrow as one voxel are detected by the above stopping criteria.

4. RESULTS AND DISCUSSION

4.1. Artificial Data

To illustrate and validate our approach, we first show results using artificial input data. Fig. 1 shows the isosurfaces of an artificially created probability map of a paraboloid-shaped layer of GM with varying thickness in a volume of 50x50x50 voxels. The two isosurfaces represent the inner and outer surfaces. Depicted as small circles, a number of sample points have been chosen, where the computed thicknesses are illustrated as line segments. The direction of each line segment is the optimal direction that gives the minimum line integral of the probability map. The thickness is demonstrated on the figure by the length of the line segments.

Next, to show the negative consequences of hard segmentation when noise and partial volume effects are present, we reduced the resolution of the volume five times by taking the mean value of every 5x5x5 sub-volume; we also added zero-mean Gaussian noise with standard deviation of 0.2 (Fig. 5(b)), and ran the measurement algorithm on it. In addition, we performed hard segmentation on the low-resolution, noisy volume by substituting the probability values less than 0.5 with 0 and other values with 1 (Fig. 5(c)), and re-ran the measurement algorithm. Using the results of the high-resolution case as ground truth, the experiments on the low resolution and noisy volumes showed an average error in the estimated thickness of 1.9 voxels in the segmentation-free case and 2.2 voxels when hard segmentation was performed for reporting this measurement.

4.2. Real MRI Data

We tested the proposed technique on 44 T1-weighted brain MRI scans, acquired using a standard sagittal 3D MP-RAGE sequence (TR: 2400 ms, minimum TE, inversion time (TI) 1000 ms, flip angle: 8°, 24 cm field of view) with a reconstructed voxel size of 0.9375x0.9375x1.2 mm^3. To adjust for scanner – and session – specific calibration errors, standard corrections were made for gradient nonlinearity, phantom-based scaling, and adjustment of intensity inhomogeneity [17].

We consider the probability of each voxel belonging to the GM as a Gaussian distribution on the intensity value of the voxel in the MRI volume. The mean of the Gaussian is the mean value of manually-selected sample voxels in the GM, while the standard deviation is the difference between the manually estimated mean values of GM and WM. We could use more sophisticated soft classification algorithms, such as Partial-Volume Bayesian algorithm (PVB) [18], Probabilistic Partial Volume Classifier (PPVC) [19], and Mixel classifier [20], to further improve the results.

Our dataset includes pairs of scans over a one-year interval from 22 subjects, of whom 9 had been diagnosed with Alzheimer's disease at their first scan, and 13 were age-matched normal subjects. The mean thickness in the temporal lobe showed an average of 1% decline over a year in the AD patients (with the standard error of 1%), and virtually no decline in the normal brains.[2] The temporal lobe, where greatest change is expected in AD, was defined by linearly aligning binary regions of interest from a standardized atlas onto the thickness map (while more sophisticated registration is possible, the mean thickness is robust to small errors in defining the limits of this relatively large region).

A 2D slice from an MRI volume is shown in Fig. 6(a) along with its computed thickness map in Fig. 6(b). Since we do not extract the GM, the results also contain thickness values for other parts of the head such as the scalp, which may be ignored. Fig. 7 illustrates a 3D surface-based mapping of the cortical thickness visualized by the mrGray software, using the steps in [21].

5. CONCLUSIONS

We presented a new definition of cortical thickness along with an algorithm for computing it. We were motivated by the importance of measuring the thickness of cerebral cortex for quantifying the progression of various neurodegenerative brain diseases. Our method calculates the thickness at each voxel, by computing all line integrals of the probability map of the gray matter passing through that voxel, and choosing the minimum integral value. Two stopping criteria are taken into consideration to address issues created by narrow sulci. Unlike most prior work, we take into account the probability of each voxel belonging to the gray matter layer and do not carry out a hard segmentation prior to measuring the thickness. We have validated the technique with artificial data and presented reasonable preliminary results for longitudinal MRI scans of Alzheimer's disease and normal subjects.

ACKNOWLEDGMENTS: This work was supported in part by the National Institutes of Health (NIH) and the National Science Foundation (NSF).

6. REFERENCES

[1] P. M. Thompson *et al*, "Abnormal cortical complexity and thickness profiles mapped in Williams syndrome," *J. Neuroscience*, vol. 25, no. 16, pp. 4146–4158, Apr. 2005.

[2] P. M. Thompson *et al*, "Mapping cortical change in Alzheimer's disease, brain development, and schizophrenia," *NeuroImage*, vol. 23, pp. 2–18, Sep. 2004.

[3] B. Fischl and A. M. Dale, "Measuring the thickness of the human cerebral cortex from magnetic resonance images," *Proc. Nat. Acad. Sci.*, vol. 97, no. 20, pp. 11 050–11 055, 2000.

[4] S. E. Jones, B. R. Buchbinder, and I. Aharon, "Three-dimensional mapping of the cortical thickness using Laplace's equation," *Hum. Brain Mapping*, vol. 11, pp. 12–32, 2000.

[5] N. Kabani, G. Le Goualher, D. MacDonald, and A. C. Evans, "Measurement of cortical thickness using an automated 3-D algorithm: a validation study," *NeuroImage*, vol. 13, no. 2, pp. 375–380, Feb. 2001.

[6] G. Lohmann, C. Preul, and M. Hund-Georgiadis, "Morphology-based cortical thickness estimation," *Inf Process Med Imaging*, vol. 2732, pp. 89–100, 2003.

[7] A. J. Yezzi and J. L. Prince, "An Eulerian PDE approach for computing tissue thickness," *IEEE Trans. Med. Imag.*, vol. 22, pp. 1332–1339, Oct. 2003.

[8] J. P. Lerch and A. C. Evans, "Cortical thickness analysis examined through power analysis and a population simulation," *NeuroImage*, vol. 24, pp. 163–173, 2005.

[9] N. Thorstensen, M. Hofer, G. Sapiro, H. Pottmann, "Measuring cortical thickness from volumetric MRI data," unpublished, 2006.

[2] The average is reported over a mask for the GM layer obtained by hard-thresholding the initial probability map which was used as the input data.

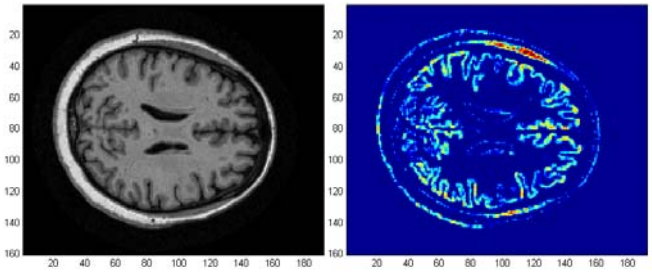

(a) (b)

Fig. 6. *Experimental results on MRI data. All computations have been done in 3D. (a) A slice of the original volume. (b) The thickness map of the same slice (blue thinner, red thicker).*

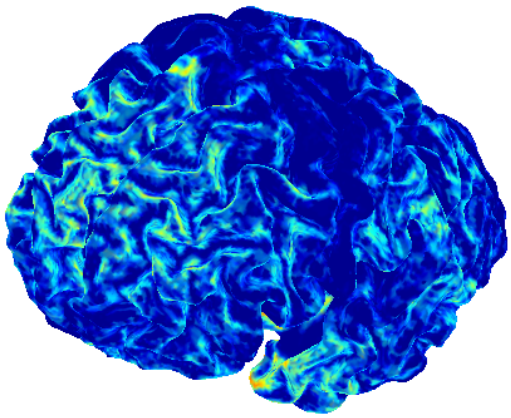

Fig. 7. *3D mapping of the cortical thickness (blue thinner, red thicker).*

[10] K. Young, N. Schuff, "Measuring structural complexity in brain images," *NeuroImage*, to be published.

[11] D. L. Pham and P. L. Bazin, "Simultaneous boundary and partial volume estimation in medical images," in *Proc. 7th Intl. Conf. Medical Image Computing and Computer-Assisted Intervention*, Saint-Malo, 2004, pp. 119–126.

[12] D. MacDonald, N. Kabani, D. Avis, and A. C. Evans, "Automated 3-D extraction of inner and outer surfaces of cerebral cortex from MRI," *NeuroImage*, vol. 12, pp. 340–356, 2000.

[13] M. I. Miller, A. B. Massie, J. T. Ratnanather, K. N. Botteron, and J. G. Csernansky, "Bayesian construction of geometrically based cortical thickness metrics," *NeuroImage*, vol. 12, pp. 676–687, 2000.

[14] M. L. J. Scott and N. A. Thacker, "Cerebral cortical thickness measurements," Imaging Science and Biomedical Engineering Division, University of Manchester, Manchester, England, TINA Memo 2004-007, 2004.

[15] H. Haidar, J. S. Soul, "Measurement of cortical thickness in 3D brain MRI data: Validation of the Laplacian method," *NeuroImage*, vol. 16, pp. 146–153, 2006.

[16] S. Pizer, D. Eberly, D. Fritsch, and B. Morse, "Zoom-invariant vision of figural shape: The mathematics of cores," *Comput. Vision Image Understanding*, vol. 69, no. 1, pp. 55-71, 1998.

[17] A. D. Leow *et al*, "Longitudinal stability of MRI for mapping brain change using tensor-based morphometry," *NeuroImage*, vol. 31, pp. 627-640, 2006.

[18] D. H. Laidlaw, K. W. Fleischer, and A. H. Barr, "Partial-volume Bayesian classification of material mixtures in MR volume data using voxel histograms," *IEEE Trans. Med. Imag.*, vol. 17, pp. 74-86, Feb. 1998.

[19] H. S. Choi, D. R. Haynor, and Y. M. Kim, "Multivariate tissue classification of MRI images for 3-D volume reconstruction—A statistical approach," in *Proc. SPIE Medical Imaging III: Image Processing*, 1989, vol. 1092, pp. 183-193.

[20] H. S. Choi, D. R. Haynor, and Y. M. Kim, "Partial volume tissue classification of multichannel magnetic resonance images—A mixel model," *IEEE Trans. Med. Imag.*, vol. 10, no. 3, pp. 395-407, 1991.

[21] P.C. Teo, G. Sapiro and B.A. Wandell, "Creating connected representations of cortical gray matter for functional MRI Visualization," *IEEE Trans. Medical Imaging*, vol. 16, no. 6, pp. 852-863, 1997.